*Design of Machines and Structures, Vol. 13, No. 1 (2023), pp. 28–38.*
*https://doi.org/10.32972/dms.2023.015*

# NEW METHOD FOR THE GEOMETRIC DESIGN OF THE RUNNER WHEEL OF THE BÁNKI TURBINE

SÁNDOR HAJDÚ
*University of Miskolc, Institute of Energy Engineering and Chemical Machinery*
*3515 Miskolc-Egyetemváros*
*hajdusor@gmail.com*
*https://orcid.org/0000-0001-5048-6932*

**Abstract:** This article is a continuation of a previous publication by Author. Paper (Hajdú, 2022) analyses the velocity relationships in the flow stream through the Bánki turbine. By exploring the velocity relationships, it is possible to determine the flow losses in the turbine runner and the runner efficiency of the runner. By implementing the theoretical results in practice, a new design procedure for the geometry of the runner of the Bánki turbine is developed.

***Keywords:*** *streamline, methodology, runner efficiency, Bánki-turbine*

## 1. INTRODUCTION

The Hungarian literature on Bánki's turbine has long lacked further development of the theory, which has stagnated since Bánki's time. In order to move forward, it was necessary to turn the research work in a completely new direction, breaking away from the available precedents in the Bánki turbine literature. Important result of this research work, beyond the results summarised in (Hajdú, 2022), is the new design procedure based on the determination of the runner efficiency of the Bánki turbine runner. The interpretation of the indices assigned to the velocity and the direction angle of the velocity on the radius circle is the same as it was given in the above-mentioned literature. Likewise, the interpretation of the $x, y$ orthogonal coordinate system and the $r, \phi$ polar coordinate system are also the same.

## 2. THE BÁNKI TURBINE IN THE PARTIAL OPENING CONDITION

Quantities for partial openings are indicated by the subscript $i$. For full closure of the waterway $i = 0$, for full opening $i = 1$. The regulating tongue is rotated by an angle $\delta_1$ from its position of full closure to its position of full opening *(Figure 1)*. In the case of partial opening, the angle of rotation of the control tongue is less than $\delta_1$, as expressed by the following relation: $\delta_i = i\delta_1; \ldots 0 \leq i \leq 1$.

The flow at the runner inlet in the partial opening condition is assumed to be

– the direction angle of the flow on the section $S_iS_0$ *(Figure 1)* of the runner circumference is equal to the direction angle $\alpha_0$,

– the central angle associated with the section $S_iS_0$ varies in proportion to the opening parameter $i$: $\varepsilon_i = i\varepsilon$; $0 \leq i \leq 1$

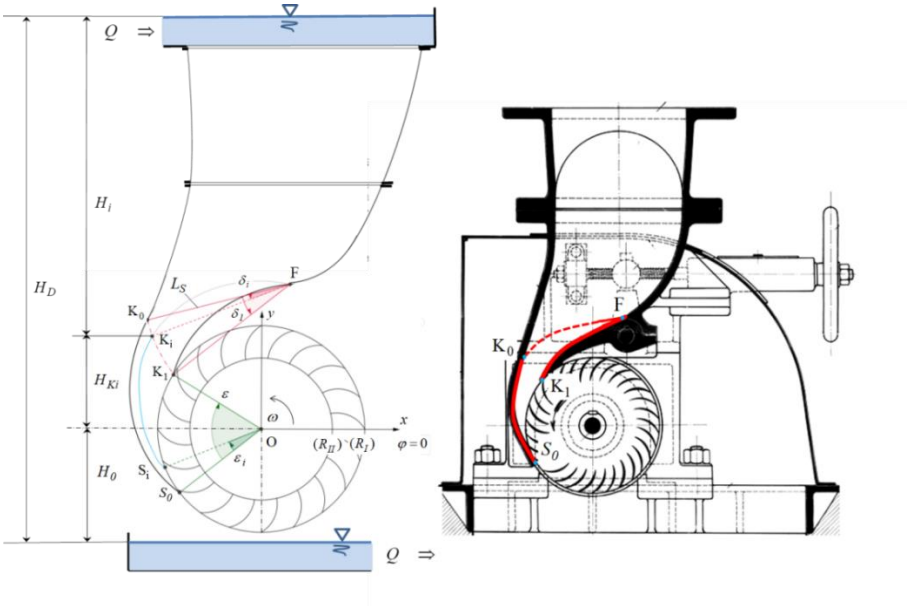



***Figure 1.*** *Schematic of the Bánki turbine in the partial opening condition*

The variation of the $H_i < H$ head as a function of the opening determines the $c_{1,i} < c_1$ flow velocity of the fluid on the runner.

$$c_{1,i} = \sqrt{2gH_i} = c_1\sqrt{H_i/H} \tag{1}$$

The flow velocity at the inlet in the direction perpendicular to the inlet surface:

$$c_{1m,i} = c_{1,i}\,sin\,\alpha_0 = sin\,\alpha_0\sqrt{2gH_i} = c_1\,sin\,\alpha_0\sqrt{H_i/H} \tag{2}$$

The volume flow rate through the runner varying as a function of the opening parameter:

$$Q_i = R_I\varepsilon_i L c_{1m,i} = R_I i\varepsilon L c_1\,sin\,\alpha_0\sqrt{H_i/H} = iQ\sqrt{H_i/H}\;;\quad 0 \leq i \leq 1 \tag{3}$$

## 3. THE EFFICIENCY SHELL DIAGRAM OF THE BÁNKI TURBINE

In paper (Hajdú, 2022), equations (16) and (17) interpret the runner efficiency for the partial opening condition as the difference between the theoretical runner power and the contraction, collision, and friction performance losses in the runner in the

partial opening condition. By combining the above equations (16) and (17), a formula is obtained to calculate the runner efficiency for the partial opening condition:

$$\eta_{jk,i} = \frac{P_{jk,i}}{P_H} = \frac{P_{E,i} - P'_{0,i} - P'_{K,i} - P'_{V,i}}{P_H} = C_{2,i}\psi^2 + C_{1,i}\psi \tag{4}$$

$$C_{2,i} = -\frac{i}{1+\cot^2\alpha_0}\left(\frac{H_i}{H}\right)^{3/2}\left[2 + \frac{2\cot\beta_1}{\psi_0} + \zeta_{K,i}\left(S_{II}^2 - \frac{1}{\psi_0^2 S_{II}^2}\right) - \frac{\zeta_{V,i}}{\psi_0^2 S_{II}\sin\beta_1}\right] \tag{5}$$

$$C_{1,i} = \frac{2i}{1+\cot^2\alpha_0}\left(\frac{H_i}{H}\right)^{3/2}\left[3\cot\beta_1 + \psi_0 - \frac{\zeta_{K,i}}{\psi_0 S_{II}^2} - \frac{\zeta_{V,i}}{\psi_0 S_{II}\sin\beta_1}\right] \tag{6}$$

The equation (4) obtained for the runner efficiency of the runner interprets a surface in the three-dimensional rectangular coordinate system $i, \psi, \eta$ and can therefore be used to construct a shell diagram of the Bánki turbine runner efficiency. This shell diagram is nothing more than the image of the surface described by the previous equation, represented by the $\eta_n = const$ level lines. The implicit equation of such a level line is:

$$C_{2,i}(i)\psi^2 + C_{1,i}(i)\psi - \eta_n = 0 \tag{7}$$

The solution of this second-degree algebraic equation (7) for $\psi$:

$$\psi_{1,2}(i) = \frac{-C_{1,i}(i) \pm \sqrt{C_{1,i}^2 + 4C_{2,i}\eta_n}}{2C_{1,i}(i)} \tag{8}$$

which provides the upper and lower sections of the level line in question in the orthogonal coordinate system *(Figure 2)*.

The interpretational range of the efficiency curve in the $i, \psi$ coordinate plane is $i_{min,n} \leq i \leq 1$; and this curve has a peak at the abscissa $i = i_{min,n}$ *(Figure 2)*. At the peak of the curve, the tangent to the curve is vertical, and the two curve segments are located to the right of this point. The equation $C_{1,i}^2 + 4C_{2,i}\eta_n = 0$ is true for the abscissa at the peak of the curve. The abscissa value can be calculated from the above equation by a series of trial-and-error operations.

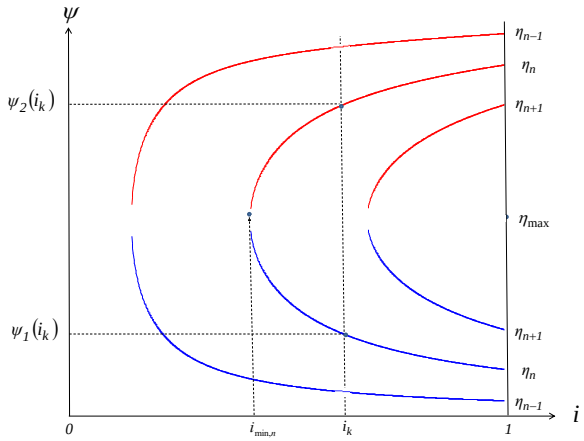



***Figure 2.*** *Level lines of the runner efficiency surface of the runner on the $i, \psi$coordinate plane*

## 4. DESIGN OF THE BÁNKI TURBINE

The design task is to determine the main geometric dimensions of the Bánki turbine that can optimally utilize the $P_D = \rho g Q H_D$ power coming from the river at a given location for a given pair of values $Q$ (flow rate to the turbine) and $H_D$ (difference in level of the dam).

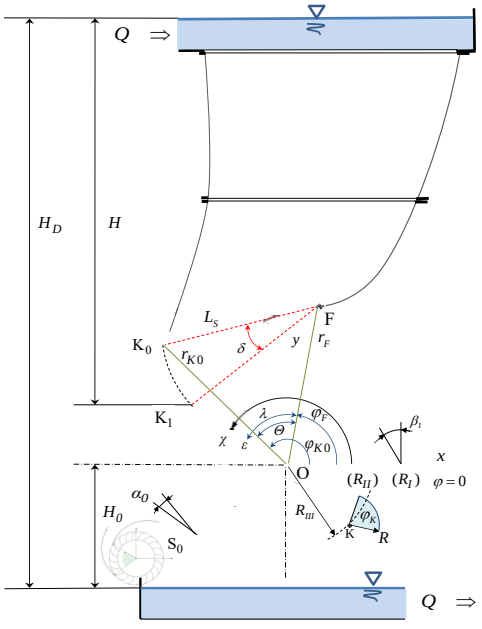



***Figure 3.*** *The angles and radii determining the installation of the Bánki turbine and the runner bladed space and the logarithmic spiral guideway walls*

The initial design data are:
(a) the volumetric flow rate of the water flow through the turbine $Q$ $(m^3/s)$;
(b) the difference in dam level at the location $H_D$ (m);
(c) the ratio of the runner radii $R_{II}/R_I = S_{II}$;
(d) the relative width of the runner $L/R_I$;
(e) the relative height of the centre of the runner above the sub-water level $H_0/R_I$;
(f) the angle of the centre of the guide tongue $\lambda$;
(g) the number of runner blades $N$;
(h) the angle of entry of the blades $\beta_1$;
(i) the angle of direction of the absolute flow defined by the guide channel $\alpha_0$;
(j) the centre angle associated with the full opening condition $\varepsilon$;
(k) the angular coordinate value defining the position of the end point of the water flow control tongue in the $r, \varphi$coordinate system at full opening $\chi$.

For notations, see the notations in *Figure 3*; $L$ is the length of the runner blade measured perpendicular to the blade.

The Bánki turbine shall be designed a) for an impact-free flow entering the runner (i.e., the operating condition $\psi_0 = cot\,\alpha_0 - cot\,\beta_1$ (Hajdú, 2022) is the design operating condition) and b) for the full opening condition of the turbine.

Using the value of the initial data (a) to (k), the main data of the Bánki turbine can be calculated using the equations listed below.

The power coming from the river:

$$P_D = \rho\, gQH_D \tag{9}$$

The size $R_I$ and the value of the available head $H$can be determined iteratively using the following two equations. The size of the inlet surface $R_I \varepsilon\, L$ at the runner peripheral face affected by the inlet is given by the ratio of the volumetric flow rate $Q$ through the runner at full opening divided by the radial (meridional) inlet velocity $c_{1m} = \sqrt{2gH}\, sin\,\alpha_0$, and hence:

$$R_{I,i+1} = \sqrt{\frac{Q}{\varepsilon\ L/R_I \sqrt{2gH_i}\, sin\,\alpha_0}} \tag{10}$$

From equation (1) in (Hajdú, 2022):

$$H_{i+1} = H_D - R_{I,i+1}(H_0/R_I + sin\,\chi) \tag{11}$$

At the beginning of the iteration $(i = 0)$ $H_0 = H_D$.

The inlet is impact-free if the runner speed in RPM is:

$$n_0 = \frac{30\sqrt{2gH}\,sin\,\alpha_0}{R_I\pi}\psi_0 = \frac{30\sqrt{2gH}}{R_I\pi}(cos\,\alpha_0 - cot\,\beta_1) \tag{12}$$

The radius of the blade arc can be calculated from *Figure 3* in (Hajdú, 2022):

$$R = \frac{R_I(1 - S_{II}^2)}{2\,cos\,\beta_1} \tag{13}$$

Centre angle of the blade arc is:

$$\varphi_k = \pi - \beta_1 - arctan\left(\frac{1 - S_{II}^2}{1 + S_{II}^2}tan\,\beta_1\right) - arctan\left(\frac{S_{II}R_I}{R}\right) \tag{14}$$

Length of the blade arc is: $L_k = R\phi_k$. Runner width is: $L = R_I(L/R_I)$.

The relative flow in the blade channels can be considered as a rectangular cross-sectional pipe flow. According to (Hajdú, 2022), the length of the pipe is: $L_{cs} = L_k N\frac{\varepsilon}{\pi}$ and the hydraulic diameter of the pipe is: $D_H = 4\frac{L\pi R_I}{LN+2\pi R_I}$. The velocity of fluid flow in the pipe is: $\bar{w} = \sqrt{\frac{2gH}{S_{II}\,sin\,\beta_1(1+cot^2\,\alpha_0)}}$. The Reynolds number of the pipe flow is: $Re = \frac{\bar{w}D_H}{\upsilon}$ , $\upsilon = 10^{-6}\ m^2/s$.

Knowing the Reynolds number, the pipe friction coefficient $\lambda_{cs}$ can be determined by a numerical approximation method taking into account that $\kappa = 0.407$. Knowing the pipe friction coefficient $\lambda_{cs}$, the friction loss factor is: $\zeta_V = \lambda_{cs}\frac{L_{cs}}{D_H}$. The contraction loss factor according to (Hajdú, 2022) is: $\zeta_K = \left(\frac{\varepsilon\,sin(\varepsilon/2)}{2(1-cos(\varepsilon/2))} - 1\right)^2$.

The runner efficiency of the Bánki turbine runner in the operating condition $\psi_0$ is:

$$\eta_{jk}(\psi_0) = 1 - \frac{1 + (\psi_0 - cot\,\beta_1)^2}{1 + cot^2\,\alpha_0} - \frac{\zeta_K(1 + S_{II}^4\psi_0^2)}{S_{II}^2(1 + cot^2\,\alpha_0)} - \frac{\zeta_V}{S_{II}\,sin\,\beta_1\,(1 + cot^2\,\alpha_0)} \tag{15}$$

The resulting efficiency in the operating condition $\psi_0$ is interpreted as the ratio of the runner power to the power coming from the river:

$$\eta_{resulting}(\psi_0) = \frac{P_{jk}(\psi_0)}{P_D} = \eta_{jk}(\psi_0)\frac{\rho\,gQH}{\rho\,gQH_D} = \eta_{jk}(\psi_0)\frac{H}{H_D} \tag{16}$$

The height difference between the centre of the runner and the sub-water level *(Figure 3)* is: $H_0 = R_I(H_0/R_I)$. The radius of the circle delimiting the inside of the runner's bladed space is: $R_{II} = S_{II}R_I$. The radius of a circle concentric with the centre of the runner and representing the geometric location of the centres of the blade arcs

*(Figure 3)* is: $R_{III} = \sqrt{R_{II}^2 + R^2}$. The angular coordinate $\varphi_F$ *(Figure 3)* of the point of rotation $F$ of the control tongue *(Figure 3)* in the coordinate system $r, \varphi$ is:$\phi_F = \chi - \lambda$. The radial coordinate $r_F$ of the rotation point $F$ of the regulating tongue *(Figure 3)* in the coordinate system $r, \varphi$ is: $r_F = R_I e^{\lambda \tan \alpha_0}$.

Length of the regulating tongue *(Figure 3)* is:

$$L_S = R_I \sqrt{1 + e^{2\lambda \tan \alpha_0} - 2e^{\lambda \tan \alpha_0} \cos \lambda} \tag{17}$$

The angle of the absolute flow leaving the runner is $\alpha_4$ [as indicated in (Hajdú, 2022)]. The following equations are obtained by taking into account equation (7) of (Hajdú, 2022) and equation $\beta_4 = \pi - \beta_1$:

$$cot\, \alpha_4 = \psi + cot\, \beta_4 = \psi - cot\, \beta_1 = (cot\, \alpha_1 - cot\, \beta_1) - cot\, \beta_1 = cot\, \alpha_1 - 2\, cot\, \beta_1 \tag{18}$$

In the impact-free entry mode ($\psi = \psi_0$) $\alpha_1 = \alpha_0$ is valid, hence, according to the (18), $cot\, \alpha_4 = cot\, \alpha_0 - 2\, cot\, \beta_1$ is satisfied. This implies that the choice of the value pair $\alpha_0; \beta_1$ in the impact-free entry mode determines the direction angle $\alpha_4$ of the absolute flow exit, and that the mode characteristic number $\psi_p$ associated with the radial exit is:

$$\psi_p = cot\, \beta_1 \quad (\alpha_4 = \pi/2, \qquad cot\, \alpha_4 = 0) \tag{19}$$

If the choice of the value pair $\alpha_0; \beta_1$ satisfies the condition $cot\, \alpha_0 = 2\, cot\, \beta_1$, then, according to the (19)

$$\psi_p = cot\, \beta_1 = \psi_0 = cot\, \alpha_0 - cot\, \beta_1 \tag{20}$$

is satisfied, i.e., the radial exit and impact-free entry occur in the same operating condition. It also follows from the above that, if $\alpha_0 = \beta_1/2$, then $\alpha_4 = \text{acot}(cot\, \alpha_0 - 2\, cot\, \beta_1) < \pi/2$ is satisfied and the angle of exit deviates only slightly from $\pi/2$.

Baseline data chosen for the design example are:

$$H_D = 3\ [m], Q\ =\ 1\ [m^3/s], L/R_I = 4, R_{II}/R_I = \frac{2}{3}, \frac{H_0}{R_I} = 1.15, N = 20, \lambda = 70°$$

For the design, we choose $\alpha_0$;$\beta_1$ value pairs, where, based on (20), one $\beta_1$ value is assigned three different $\alpha_0$ values for which the following equations are satisfied:

$$\alpha_0 = \text{acot}(2\, cot\, \beta_1) \rightarrow \alpha_4 = \text{acot}(cot\, \alpha_0 - 2\, cot\, \beta_1) = \frac{\pi}{2}$$

$$\alpha_0 < \text{acot}(2\, cot\, \beta_1) \rightarrow \alpha_4 = \text{acot}(cot\, \alpha_0 - 2\, cot\, \beta_1) < \frac{\pi}{2} \leftarrow \alpha_0 = \frac{\beta_1}{2}$$

$$\alpha_0 > \text{acot}(2\, cot\, \beta_1) \rightarrow \alpha_4 = \text{acot}(cot\, \alpha_0 - 2\, cot\, \beta_1) > \pi/2 \leftarrow \alpha_0 = 1{,}1\text{acot}(2\, cot\, \beta_1)$$

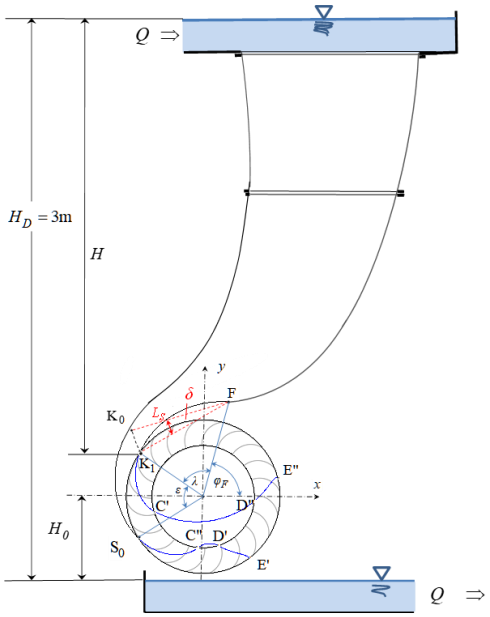



***Figure 4.*** *Scale drawing of the Bánki turbine*

Given the data of the Bánki turbine variants using the different $\alpha_0; \beta_1$ value pairs, a decision can be made on the variant to be implemented. The results of the calculations are easy to review when the data are tabulated. The results of a sample calculation are shown in *Table 1*. In the calculation example, the data in Table 1 are used to select the variant "c" in the case of $\beta_1 = 20°$ for the Bánki turbine to be implemented in order to achieve a high resulting efficiency, and the Bánki turbine is thus designed. Based on the data determined in the design, a scale plan of the Bánki turbine *(Figure 4)* and a shell diagram of the runner efficiency of the Bánki turbine runner *(Figure 5)* can be drawn.

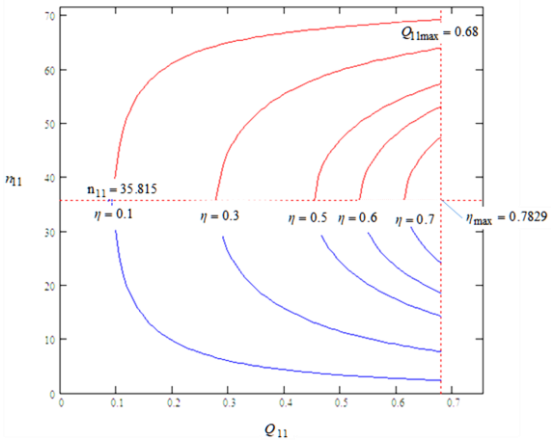



***Figure 5.*** *Shell diagram of the runner efficiency of the Bánki turbine runner*

***Table 1***
*Calculated results*

| | **a** | **b** | **c** | **a** | **b** | **c** |
|---|---|---|---|---|---|---|
| $\beta_1$° | 15 | | | 20 | | |
| $\alpha_0$° | 7.5 | 7.631 | 8.394 | 10 | 10.314 | 11.346 |
| $\varepsilon$ ° | 45 | 47 | 55 | 56 | 59 | 68 |
| $\chi$° | 147 | 147 | 150 | 151 | 150 | 145 |
| | | | | | | |
| $\psi_t = \psi_0$ | 3.8637 | 3.7321 | 3.0450 | 2.9238 | 2.7475 | 2.2364 |
| $\eta_E(\psi_0)$ | 0.9827 | 0.9824 | 0.9686 | 0.9689 | 0.9679 | 0.9512 |
| $\alpha_4(\psi_0)$° | 82.5000 | 90.0000 | 124.4911 | 80.0000 | 90.0000 | 117.0694 |
| $\varphi_C$° | 78.9424 | 76.8471 | 65.9123 | 62.4776 | 59.6713 | 51.5377 |
| $\alpha_C$° | 30.2141 | 31.0851 | 36.4613 | 37.5799 | 39.3152 | 45.1733 |
| $\varphi_D$° | 139.3705 | 139.0174 | 138.8349 | 137.6374 | 138.3016 | 141.8843 |
| $(\varphi_D - \varphi_C)$° | 60.4281 | 62.1703 | 72.9226 | 75.1598 | 78.6303 | 90.3467 |
| $\varphi_E$° | 183.4135 | 180.9651 | 169.8478 | 168.2273 | 166.0852 | 161.5342 |
| $\varphi_{K2}$° | 15.4135 | 14.9651 | 14.8478 | 15.2273 | 15.0852 | 14.5342 |
| $R_I$ m | 0.6291 | 0.6075 | 0.5249 | 0.4719 | 0.4514 | 0.3986 |
| H m | 1.9339 | 1.9705 | 2.1339 | 2.2286 | 2.2551 | 2.3129 |
| $R_{II}$ m | 0.4194 | 0.4050 | 0.3499 | 0.3146 | 0.3010 | 0.2658 |
| $R$ m | 0.1809 | 0.1747 | 0.1510 | 0.1395 | 0.1334 | 0.1178 |
| $R_{III}$ m | 0.4568 | 0.4411 | 0.3811 | 0.3441 | 0.3292 | 0.2907 |
| $\varphi_K$° | 92.4497 | 92.4497 | 92.4497 | 85.9439 | 85.9439 | 85.9439 |
| $L_k$ m | 0.2919 | 0.2819 | 0.2436 | 0.2092 | 0.2002 | 0.1768 |
| $L$ m | 2.5165 | 2.4299 | 2.0996 | 1.8875 | 1.8057 | 1.5946 |
| $\varphi_F$° | 77.0000 | 77.0000 | 80.0000 | 81.0000 | 80.0000 | 75.0000 |
| $r_F$ m | 0.7389 | 0.7155 | 0.6286 | 0.5853 | 0.5638 | 0.5094 |
| $L_S$ m | 0.7898 | 0.7640 | 0.6671 | 0.6135 | 0.5896 | 0.5287 |
| Θ° | 66.3442 | 66.1137 | 65.0009 | 64.0709 | 63.4416 | 61.6672 |
| $\varphi_{K0}$° | 143.3442 | 143.1137 | 145.0009 | 145.0709 | 143.4416 | 136.6672 |
| $r_{K0}$ m | 0.7035 | 0.6842 | 0.6126 | 0.5710 | 0.5559 | 0.5208 |
| $\delta$° | 6.2180 | 6.6287 | 8.6573 | 10.5396 | 11.6029 | 15.1030 |
| $L_{cs}$ m | 1.4596 | 1.4721 | 1.4885 | 1.3019 | 1.3122 | 1.3356 |
| $D_H$ m | 0.3665 | 0.3539 | 0.3058 | 0.2749 | 0.2630 | 0.2322 |
| $\overline{w}$ m/s | 1.9356 | 1.9877 | 2.2739 | 2.4046 | 2.4941 | 2.7753 |
| Re | 709393 | 703439 | 695337 | 661047 | 655917 | 644527 |
| $\lambda_{cs}$ | 0.0152 | 0.0152 | 0.0152 | 0.0154 | 0.0154 | 0.0154 |
| $\zeta_V$ | 0.0604 | 0.0632 | 0.0741 | 0.0728 | 0.0768 | 0.0888 |
| $\zeta_K$ | 0.9491 | 0.9446 | 0.9244 | 0.9217 | 0.9132 | 0.8854 |

| $\eta_{jk}(\psi_0)$ | 0.8330 | 0.8353 | 0.8340 | 0.7912 | 0.7931 | 0.7829 |
|---|---|---|---|---|---|---|
| $P_{jk}(\psi_0)$ kW | 15.8036 | 16.1478 | 17.4582 | 17.2965 | 17.5450 | 17.7626 |
| $n_0$ f/p | 47.1520 | 48.4379 | 52.3227 | 67.9381 | 69.2174 | 70.9942 |
| $\eta_{resulting}(\psi_0)$ | 0.5370 | 0.5487 | 0.5932 | 0.5877 | 0.5962 | 0.6036 |
| | | | | | | |
| | **a** | **b** | **c** | **a** | **b** | **c** |
| $\beta_1$° | 25 | | | 30 | | |
| $\alpha_0$° | 12.5 | 13.124 | 12.5 | 13.124 | 12.5 | 13.124 |
| $\varepsilon$ ° | 65 | 70 | 65 | 70 | 65 | 70 |
| $\chi$° | 148 | 144 | 148 | 144 | 148 | 144 |
| | | | | | | |
| $\psi_t = \psi_0$ | 2.3662 | 2.1445 | 2.3662 | 2.1445 | 2.3662 | 2.1445 |
| $\eta_E(\psi_0)$ | 0.9509 | 0.9484 | 0.9509 | 0.9484 | 0.9509 | 0.9484 |
| $\alpha_4(\psi_0)$° | 77.5000 | 90.0000 | 77.5000 | 90.0000 | 77.5000 | 90.0000 |
| $\varphi_C$° | 52.1815 | 48.6532 | 52.1815 | 48.6532 | 52.1815 | 48.6532 |
| $\alpha_C$° | 43.5580 | 46.3751 | 43.5580 | 46.3751 | 43.5580 | 46.3751 |
| $\varphi_D$° | 139.2975 | 141.4034 | 139.2975 | 141.4034 | 139.2975 | 141.4034 |
| $(\varphi_D - \varphi_C)$° | 87.1160 | 92.7503 | 87.1160 | 92.7503 | 87.1160 | 92.7503 |
| $\varphi_E$° | 162.4345 | 161.0120 | 162.4345 | 161.0120 | 162.4345 | 161.0120 |
| $\varphi_{K2}$° | 15.4345 | 15.0120 | 15.4345 | 15.0120 | 15.4345 | 15.0120 |
| $R_I$ m | 0.3872 | 0.3636 | 0.3872 | 0.3636 | 0.3872 | 0.3636 |
| H m | 2.3495 | 2.3682 | 2.3495 | 2.3682 | 2.3495 | 2.3682 |
| $R_{II}$ m | 0.2581 | 0.2424 | 0.2581 | 0.2424 | 0.2581 | 0.2424 |
| $R$ m | 0.1187 | 0.1114 | 0.1187 | 0.1114 | 0.1187 | 0.1114 |
| $R_{III}$ m | 0.2841 | 0.2668 | 0.2841 | 0.2668 | 0.2841 | 0.2668 |
| $\varphi_K$° | 79.5223 | 79.5223 | 79.5223 | 79.5223 | 79.5223 | 79.5223 |
| $L_k$ m | 0.1647 | 0.1547 | 0.1647 | 0.1547 | 0.1647 | 0.1547 |
| $L$ m | 1.5489 | 1.4543 | 1.5489 | 1.4543 | 1.5489 | 1.4543 |
| $\varphi_F$° | 78.0000 | 74.0000 | 78.0000 | 74.0000 | 78.0000 | 74.0000 |
| $r_F$ m | 0.5077 | 0.4834 | 0.5077 | 0.4834 | 0.5077 | 0.4834 |
| $L_S$ m | 0.5227 | 0.4956 | 0.5227 | 0.4956 | 0.5227 | 0.4956 |
| $\Theta$° | 61.4249 | 60.2348 | 61.4249 | 60.2348 | 61.4249 | 60.2348 |
| $\varphi_{K0}$° | 139.4249 | 134.2348 | 139.4249 | 134.2348 | 139.4249 | 134.2348 |
| $r_{K0}$ m | 0.5147 | 0.5030 | 0.5147 | 0.5030 | 0.5147 | 0.5030 |
| $\delta$° | 15.8289 | 18.2592 | 15.8289 | 18.2592 | 15.8289 | 18.2592 |
| $L_{cs}$ m | 1.1896 | 1.2030 | 1.1896 | 1.2030 | 1.1896 | 1.2030 |
| $D_H$ m | 0.2256 | 0.2118 | 0.2256 | 0.2118 | 0.2256 | 0.2118 |
| $\overline{w}$ m/s | 2.7685 | 2.9159 | 2.7685 | 2.9159 | 2.7685 | 2.9159 |
| Re | 624521 | 617625 | 624521 | 617625 | 624521 | 617625 |

| | | | | | | |
|---|---|---|---|---|---|---|
| $\lambda_{cs}$ | 0.0155 | 0.0156 | 0.0155 | 0.0156 | 0.0155 | 0.0156 |
| $\zeta_V$ | 0.0819 | 0.0883 | 0.0819 | 0.0883 | 0.0819 | 0.0883 |
| $\zeta_K$ | 0.8951 | 0.8788 | 0.8951 | 0.8788 | 0.8951 | 0.8788 |
| $\eta_{jk}(\psi_0)$ | 0.7386 | 0.7377 | 0.7386 | 0.7377 | 0.7386 | 0.7377 |
| $P_{jk}(\psi_0)$ kW | 17.0227 | 17.1388 | 17.0227 | 17.1388 | 17.0227 | 17.1388 |
| $n_0$ f/p | 85.7510 | 87.1758 | 85.7510 | 87.1758 | 85.7510 | 87.1758 |
| $\eta_{resulting}(\psi_0)$ | 0.5784 | 0.5824 | 0.5784 | 0.5824 | 0.5784 | 0.5824 |

## 5. SUMMARY

Under the conditions of a circular curve of the runner blade (the tangent to the blade is radial at the inner boundary of the bladed space) and congruent relative flow, the geometry of the runner of the Bánki turbine can be designed and a scale drawing of the turbine installation can be prepared by applying the relationships summarized in the paper. Furthermore, the expected operating data of the designed turbine can be determined, including a shell diagram of the runner efficiency of the runner. Such a calculation has not been reported in the literature so far.

## ACKNOWLEDGEMENT

This research was supported by the European Union and the State of Hungary, co-financed by the European Social Fund in the framework of TÁMOP-4.2.4.A/2-11/1-2012-0001 ‘National Excellence Program’.

## REFERENCES

Bánki, D. (1920). *Energiaátalakulások folyadékokban*. 2. kiad. Budapest: Franklin.

Czibere, T. (2009). Az el nem évülő Bánki-turbina létrehozója 150 éve született. *GÉP*, 60 (3), 9–15.

Hajdú, S. (2022). Calculation of the flow generated in the runner of a Bánki turbine. *Design of Machines and Structures*, 12 (1), 12–25. https://doi.org/10.32972/dms.2022.002

Mockmore, C., & Merryfield, F. (1949). *The Banki Water Turbine*. Engineering Station Bulletin Series, 25